



Missouri University of Science and Technology
Scholars' Mine


UMR-MEC Conference on Energy

09 Oct 1975

Direct AC Generation from Solar Cell Arrays

Fernando L. Alvarado

Follow this and additional works at: <https://scholarsmine.mst.edu/umr-mec>

 Part of the [Electrical and Computer Engineering Commons](#), [Mechanical Engineering Commons](#), [Mining Engineering Commons](#), [Nuclear Engineering Commons](#), and the [Petroleum Engineering Commons](#)

Recommended Citation

Alvarado, Fernando L., "Direct AC Generation from Solar Cell Arrays" (1975). *UMR-MEC Conference on Energy*. 86.

<https://scholarsmine.mst.edu/umr-mec/86>

This Article - Conference proceedings is brought to you for free and open access by Scholars' Mine. It has been accepted for inclusion in UMR-MEC Conference on Energy by an authorized administrator of Scholars' Mine. This work is protected by U. S. Copyright Law. Unauthorized use including reproduction for redistribution requires the permission of the copyright holder. For more information, please contact scholarsmine@mst.edu.

DIRECT AC GENERATION FROM SOLAR CELL ARRAYS

Fernando L. Alvarado
The University of Wisconsin

Adel H. Eltimsahy
The University of Toledo

Abstract

Results of the investigation of the performance of solar cells when directly coupled to a conventional three-phase power network are presented. This approach dissociates the electricity production problem from the electric energy storage problem. Extensive studies of the required power inverter are performed. Preliminary simulation results indicate that ac power outputs of better than 90% of the optimum cell power output can be easily achieved by means of a suitably controlled inverter, thereby justifying the elimination of dc loads or local dc electric energy storage devices. It is also shown that the controlling policy for the inverter must depend on the operating conditions of the system, such as cell temperature, solar intensity and power system voltage variations, otherwise the performance of the inverter can deteriorate quite dramatically.

INTRODUCTION

It appears likely that the cost of solar cells will drop in the next few years; it is, therefore, pertinent to investigate the possibility of utilizing solar cells for bulk generation of electricity on earth-based facilities. Since solar cells are inherently dc devices, three alternatives appear feasible: direct utilization of the dc power, storage of dc electric energy and direct connection to the power network.

The direct utilization of the dc power through inverters requires the selection of a suitable useful dc load [1]. As the operating conditions vary, so do the optimal load characteristics. This method has other limitations, such as the location and type of load that can be used.

Furthermore, the power available to the load is of an intermittent nature.

The storage of dc electric energy can be accomplished by a variety of means, such as electrochemical storage (batteries), or fuel cells. This eliminates the shortcomings due to the intermittent nature of the source. There are still limitations as to useful load location and type. Moreover, the overall efficiency of the system is reduced and its cost increased.

The third alternative, connection to the power network through inverters offers a great amount of flexibility and high efficiency at the expense of inverter circuit complexity. This approach places solar cells in the same category as "off the river" hydro plants to the extent that power is supplied to the network on an

"as available" basis. The problem of energy storage is not eliminated, but it can be studied independently of the detailed study of solar generators/power inverters. A companion paper [9] studies the coincidence factor between solar insolation and electric demand for a specific region of the country. It is encouraging to notice that there is generally good correlation between peak electric demand and solar intensity.

MODELING SOLAR CELLS

Voltage-current relationships for solar cells are well-established from both theoretical and experimental considerations [2-6]. For the studies to be undertaken in this paper the following mathematical model has been chosen, based primarily on [5]:

$$E = K_e T \ln[1 + (I_s - I)/I_o] \quad (1)$$

$$I_o = K_o T^4 A \exp[-E_g/(K_e T)] \quad (2)$$

$$I_s = K_s A G \quad (3)$$

$$V = E - I R_i \quad (4)$$

where

E - internal light-induced cell voltage (V)

I - cell current (A)

T - temperature ($^{\circ}$ K)

I_s - ideal ($R_i = 0$) cell short-circuit current (A)

I_o - maximum reverse-current (A)

V - cell terminal voltage (V)

R_i - internal series resistance (Ω)

A - cell area (m^2)

G - energy density (W/m^2)

E_g - energy gap of material (eV)

K_e , K_o and K_s - proportionality constants (K_o and K_s depend also on material properties).

The incident radiation is characterized in this model by the total solar energy density G . For this reason the "constant" K_s depends on the shape of the solar spectrum density, since I_s depends actually on

n_{ph} , the photon rate of flow per unit area for photons with an energy content greater than the energy gap E_g in the semiconductor junction. Larger values of n_{ph} (like those achieved by means of concentrators) tend to increase the importance of the losses in the internal cell resistance R_i [3,4,7]. Important dynamic effects appear if temperature variations are considered. The present paper neglects thermal dynamics and assumes constant temperature. Higher temperatures (often the result of larger G) result in reduced voltages and powers.

To illustrate the typical relationships obtained from (1) to (4) a silicon solar cell with the following parameters was chosen [6]:

$$\begin{aligned} K_e &= 8.617 \times 10^{-5} & E_g &= 1.11 \text{ eV} \\ K_o &= 275 & A &= 2 \times 10^{-4} \text{ m}^2 \\ K_s &= 4.28 \times 10^{-2} & R_i &= .4 \text{ ohm} \end{aligned}$$

(Note: Under the solar conditions and energy gap chosen $G = 1 \text{ W/m}^2$ corresponds to $n_{ph} = 7.20 \times 10^{17}$ photons/ m^2 .)

The E-I curves for this cell were obtained for a variety of incident radiation levels G and cell temperature T combinations. The results are illustrated in Figure 1.

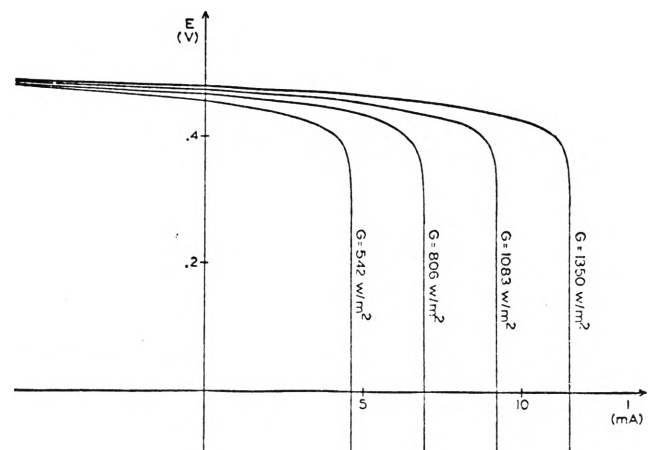


Fig. 1a. Voltage-current characteristics of cells. Variations in G with $T = 300^{\circ}$ K.

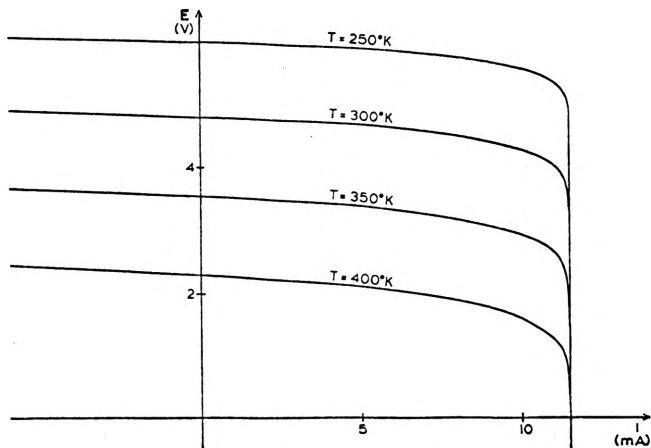


Fig. 1b. Voltage-current characteristics of cells. Variations in T with $G = 1350 \text{ w/m}^2$.

THE INVERTER

This paper considers the use of controlled rectifiers to convert from ac power to dc power. This technology has been extensively studied and developed in connection with dc power transmission lines [8]. The specific configuration used in this report is the one for a three-phase full-wave rectifier/inverter using six controlled rectifiers as illustrated in Figure 2. Ideal controlled rectifiers are considered. The ideal controlled rectifier is a memory binary element with two states: "on" ($g = 1$) and "off" ($g = 0$). The "on" state is reached under the presence of an appropriate control pulse $p = 1$; the "off" state

is reached by attempting to circulate a negative current. For simulation purposes an ideal controlled rectifier can be mathematically modeled as follows:

$$g(t + dt) = \begin{cases} 0 & \text{if } g(t) = 0 \text{ and } v(t) \leq 0 \\ 1 & \text{if } g(t) = 1 \text{ and } i(t) \leq 0 \end{cases} \quad (5)$$

$$\begin{cases} g(t) = 0 \Rightarrow i(t) = 0 \\ g(t) = 1 \Rightarrow v(t) = 0 \end{cases} \quad (6)$$

The model for the active component within the dc source (the solar cell) has been described in the previous section. It is assumed that a low-pass filter in the form of a simple series inductor is used. The series resistance of the cells is combined with the inductor resistance into an overall series resistance R_d . The model for the dc source is also illustrated in Figure 2. The presence of L_d introduces a dynamic equation for I_d and (4) must be replaced by

$$\dot{I}_d = (E_d - V_d - R_d I_d) / L_d \quad (7)$$

The three-phase ac system is modeled by inductive impedances in series with ideal sinusoidal voltage sources. The model for this system is illustrated in Figure 2 and it can be described mathematically as:

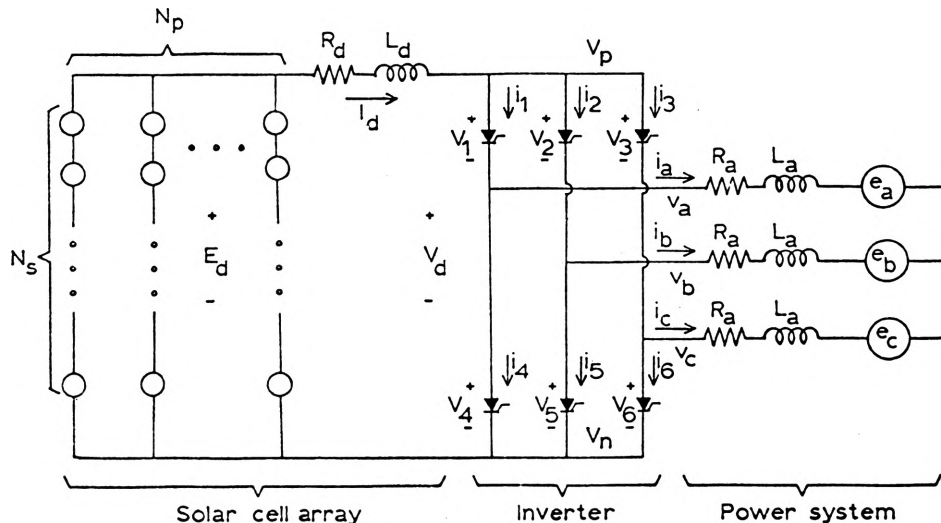


Fig. 2. The cell/inverter/power system equivalent circuit. Voltages V_p , V_n , V_a , V_b and V_c are defined with respect to power system neutral.

$$\begin{aligned} \dot{i}_a &= (v_a - e_a - R_a i_a) / L_a \\ \dot{i}_b &= (v_b - e_b - R_a i_b) / L_a \\ \dot{i}_c &= (v_c - e_c - R_a i_c) / L_a \end{aligned} \quad (8)$$

$$\begin{aligned} e_a &= E_a \sqrt{2} \sin(\omega t - \theta_a) \\ e_b &= E_a \sqrt{2} \sin(\omega t - \theta_a - 120^\circ) \\ e_c &= E_a \sqrt{2} \sin(\omega t - \theta_a - 240^\circ) \end{aligned} \quad (9)$$

where

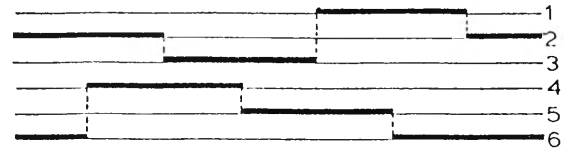
E_a - effective line to neutral voltage
 θ_a - phase angle

THE SIMULATION STUDY: GENERAL

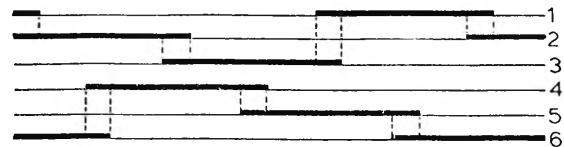
The successful design and operation of the solar electric generator described in the previous sections involves such considerations as the adequate design, orientation and location of solar cells, the design of adequate concentrators, the selection of circuit parameters (inductors, etc.) and the selection of the number of series cells and parallel paths within an array. One of the most fundamental considerations, however, is the appropriate timing of the control pulses p to the controlled rectifiers. The remainder of this paper is devoted primarily to the study of controlled rectifier control policies. The following notation is adopted for all further discussions:

- α - ignition delay in electrical degrees (e.g., delay between the time when conduction would start in an uncontrolled rectifier, $v > 0$ and the time when the corresponding pulse p is applied to the rectifier).
- u - overlap angle (time in electrical degrees between the beginning of conduction of a given controlled rectifier and the termination of conduction of another rectifier directly in parallel with it).
- $\delta = \alpha + u$ - extinction angle.

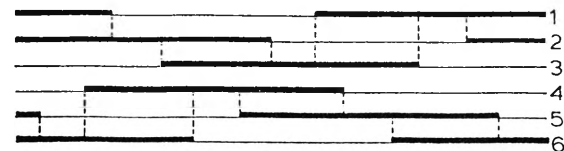
Kimbarck [8] has performed detailed analytical studies of these three-phase inverters. One of the limitations of these analytical studies is that for mathematical convenience the dc source is modeled as a constant current source for all commutation studies, although slow long term variations are allowed.



(a) No overlap ($u=0$)



(b) Single overlap ($0 < u < 60^\circ$)



(c) Double overlap ($u > 60^\circ$)

Fig. 3. Rectifier conduction sequence (solid line denotes "on" state of rectifier).

Under ideal conditions conduction in one rectifier ceases when one in parallel with it is fired. This situation arises when $L_a = 0$ and implies $u = 0$ [8]. Figure 3a illustrates the typical conduction sequence under these circumstances. The voltage V_d waveforms for various ignition delay angles α for the same case are illustrated in Figure 4. It can be observed that the average value of V_d positive is positive only when $\alpha > 90^\circ$. This means that if $\alpha \leq 90^\circ$ power cannot be delivered by the dc source but is instead absorbed by it, an obviously undesirable situation. Also, α is further restricted

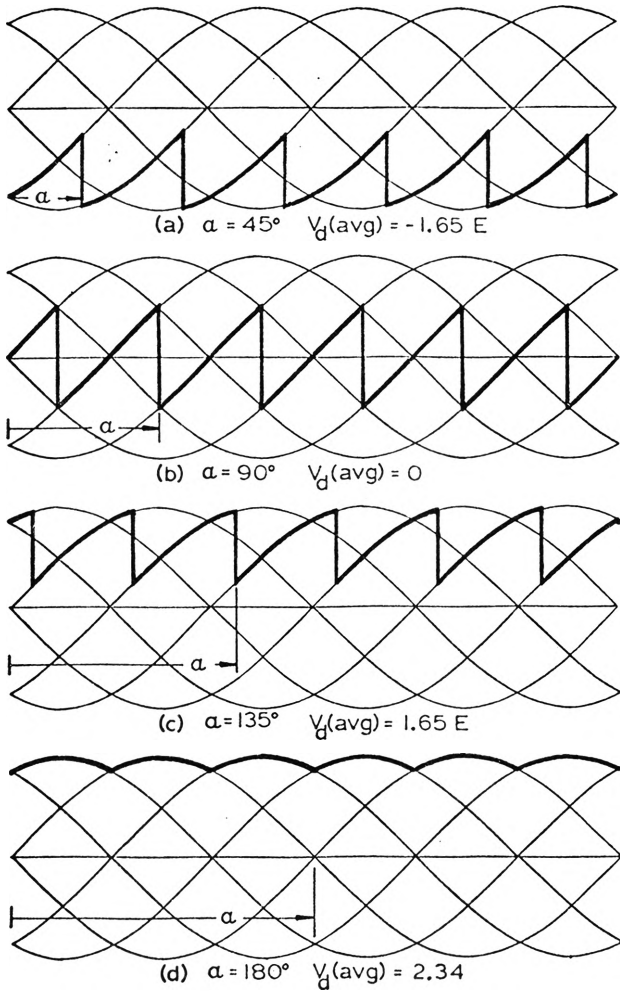


Fig. 4. V_d waveforms, no overlap.

to less than 180° , otherwise conduction in the previous valve cannot cease naturally. The presence of an inductance in the ac system alters the commutation sequence so that three rectifiers can be conducting at once, as illustrated in Figure 3b. This situation occurs when $L_a > 0$ and results in $u = \cos^{-1} (\cos \alpha - I_d / I_{s2}) - \alpha$, where $I_{s2} = \sqrt{3}E_a / \sqrt{2}\omega L_a$. In fact, if either L_a or I_d become sufficiently large or E_a sufficiently small, an abnormal condition in which four rectifiers conduct at once can develop, as illustrated in Figure 4c. This abnormal situation is not discussed herein. A further effect due to the presence of L_a is a resistive drop in the average value of V_d , even if R_a is zero. Also, δ must be restricted to less than 180° for

proper operation.

Three modes of control for controlled rectifiers are traditionally recognized: constant ignition angle α control (CIA), constant current I_d control (CCC), and constant extinction angle δ control (CEA). In the absence of L_a , CIA and CEA are equivalent. Adjusting α or δ under these conditions results in a change in V_d with a corresponding change in I_d according to (1) and (4). The presence of an inductance L_a affects the CIA to the extent that V_d will become somewhat current dependent. More important, however, is its effect on CEA, when a nonzero u means that the rectifier must be triggered in advance of the desired extinction, and this angle must be based on computed predicted values of the current; this problem becomes more critical when values of δ close to 180° must be chosen, since δ should never exceed 180° . CCC is based on adjustments of the ignition angle α based on deviations of the actual current I_d from a desired value of current. Proper design of gains and time constants in the feedback loop should be made to prevent possible control loop instabilities.

Rectifier/inverter systems are generally controlled by setting the rectifier in a CCC mode (current approximately constant); or alternately, the rectifier in a CCC mode and the inverter in a CEA mode. The choice is usually dependent on the operating conditions. It is, hence, interesting to notice that the solar cell characteristics under fixed operating conditions as illustrated in Figure 1 closely resemble the characteristics of three-phase rectifiers with one approximately constant current segment and one approximately constant voltage segment.

The simulated experimental setup used in connection with the present research was implemented in a digital computer using a continuous system modeling program.

Equations (1) - (3) and (5) - (9) were used in addition to all the necessary binary logic for the control of the rectifiers. A block diagram for each of the two possible operating configurations (two rectifiers conducting or three rectifiers conducting) was implemented as illustrated in Figure 5.

Other portions of the model, not illustrated in Figure 5, are used to control the transition between model configurations and to re-evaluate model parameters at the appropriate intervals. The ignition

pulses can be controlled by either one of the three control modes already described, or by a fourth mode, constant ratio control (CRC). Another portion of the model is used to simulate the behavior of the ignition timing controller. Only simple integral-error feedback controllers were considered in this study, although some nonlinear gains were used in an attempt to linearize the effect of control signal errors. The equations that describe the dynamics of the ignition delay angle α each of the four control modes are:

Constant Ignition Angle:

$$\alpha = \alpha_{\text{set}} \quad (10)$$

Constant Extinction Angle:

$$\alpha = \cos^{-1} (\cos \delta_{\text{set}} + I_d/I_{s2}) \quad (11)$$

Constant Current Control:

$$\dot{\alpha} = \begin{cases} 0 & \text{if } I_d > I_{\text{set}} \text{ and} \\ & \cos \alpha \geq I_d/I_{s2} - 1 \\ K_c (I_d - I_{\text{set}})/\sin \alpha & \text{otherwise} \end{cases} \quad (12)$$

Constant Ratio Control:

$$\alpha = \begin{cases} 0 & \text{if } R_{\text{set}} > V_d/I_d \text{ and} \\ & \cos \alpha \geq I_d/I_{s2} - 1 \\ K_r (R_{\text{set}} - V_d/I_d)/\sin \alpha & \text{otherwise} \end{cases} \quad (13)$$

where

$$I_{s2} = \sqrt{3} E_a / \sqrt{2} \cos L_a$$

$$V_o = 3\sqrt{6} E_a / \pi$$

The purpose of the Constant Ratio Control mode is to provide an easily implemented control mode such that the inverter efficiency is less sensitive to errors in the determination of the operating conditions, as illustrated in this next section.

A possible modification to CEA control that could be of practical interest involves the use of a feedback error signal from the desired δ to adjust α rather than the predictive formula (13). The error signal, however, could be determined

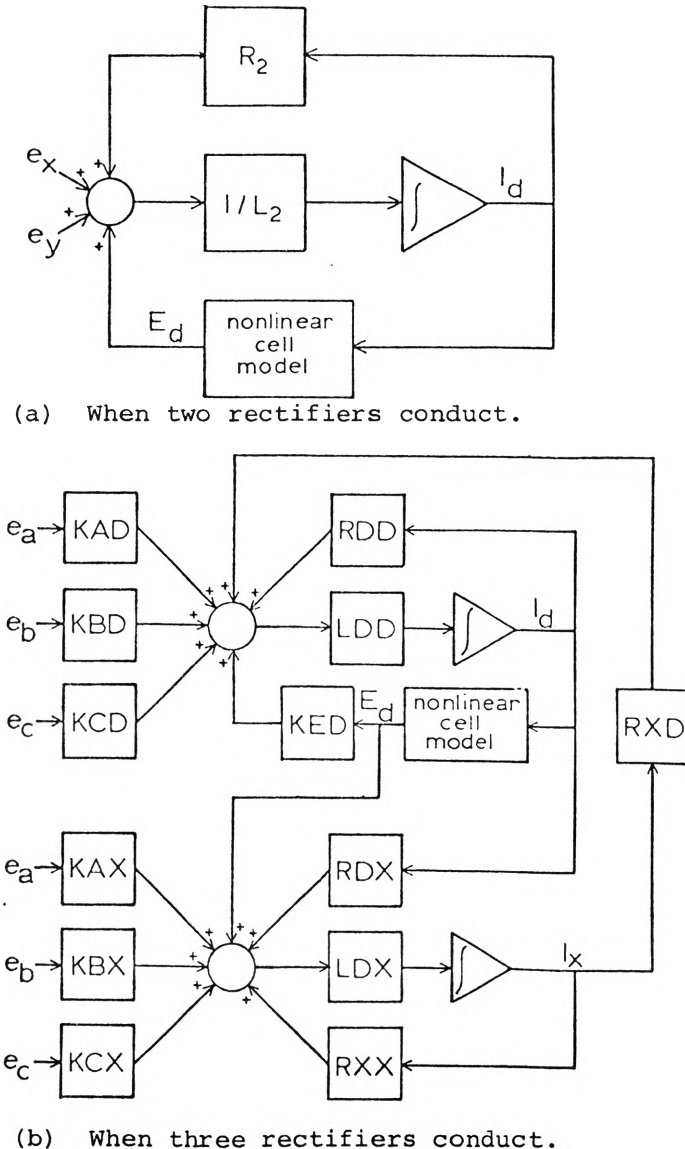


Fig. 5. Block diagram of model. Parameter values depend on which rectifiers are conducting.

only at discrete intervals. Other likely straightforward modifications include the use of a predictive term \dot{I}_d in (11) and of more complex dynamic characteristics in (12) and (13).

Another feature of the simulated model is its capability of measuring efficiencies. Three different efficiencies are defined and evaluated:

$$\eta_{cell}^* = \frac{p^*}{GA} \quad (14)$$

$$\eta_{cell} = \frac{V_d I_d}{GA} \quad (15)$$

$$\eta_{inv} = \frac{\eta_{cell}}{\eta_{cell}^*} \quad (16)$$

where:

p^* is the maximum power that the solar cell array can deliver under the given conditions of temperature and incident radiation. This number is calculated by the model via Newton iterations

GA represents the total incident power
 η_{cell}^* represents the maximum efficiency that the solar cell array is capable of operating at.

η_{cell} represents the actual efficiency under the conditions and control policies used

η_{inv} represents the efficiency due to performance deviation from the optimal by the presence of the inverter circuitry. This is the number that measures the effectiveness of the inverter.

THE SIMULATION STUDY: AN EXAMPLE

The digital model described in the previous section can be used to answer a variety of questions about the performance of any particular solar cell array under various operating conditions and control modes. This section outlines some of the most important experiments that have been performed with this model or with some variations of it, and presents the results

of a few of these experiments as performed for a specific solar cell array. These experiments include: the determination of the steady state waveforms for the various currents and voltages for specific sets of parameters, operating conditions and control modes; the determination of the instantaneous and average inverter efficiencies under steady state conditions; the determination of the effect of variations of the inverter control parameter (α_{set} , δ_{set} , I_{set} or R_{set}) as well as variations of the operating conditions (G , E and T) on the inverter efficiency. These studies can be useful in selecting optimal control parameter settings and predicting the performance degradation in case of erroneous determination of the operating conditions for the various control modes. The determination of the effect of parameter variations (L_d , L_a , N_p , N_s) on the performance of the system under CRC mode was also undertaken, as well as the study of the transient behavior of the system under sudden variations of the operating conditions.

An array of the same cells described earlier in this paper was used. The following additional system parameters were chosen for the simulation.

System Parameters:

$$\begin{aligned} R_d &= 26.1 \text{ ohm} & R_a &= .3 \text{ ohm} \\ L_d &= 1 \text{ henry} & L_a &= .3 \text{ henry} \\ N_p &= 4 & N_s &= 260 \\ (\omega) &= 377 \text{ rad/sec (60 Hz)} \end{aligned}$$

Control Parameters:

$$\begin{aligned} \alpha_{set} &= 137^\circ & I_{set} &= 45.5 \text{ mA} \\ \delta_{set} &= 144^\circ & R_{set} &= 3000 \text{ ohm} \end{aligned}$$

Operating Conditions (basic study):

$$T = 300 \text{ K} \quad G = 1350 \text{ w/m}^2 \quad E = 49 \text{ volts}$$

Figure 6 illustrates some of the steady-state waveforms obtained. The comparatively large variations in E_d for small

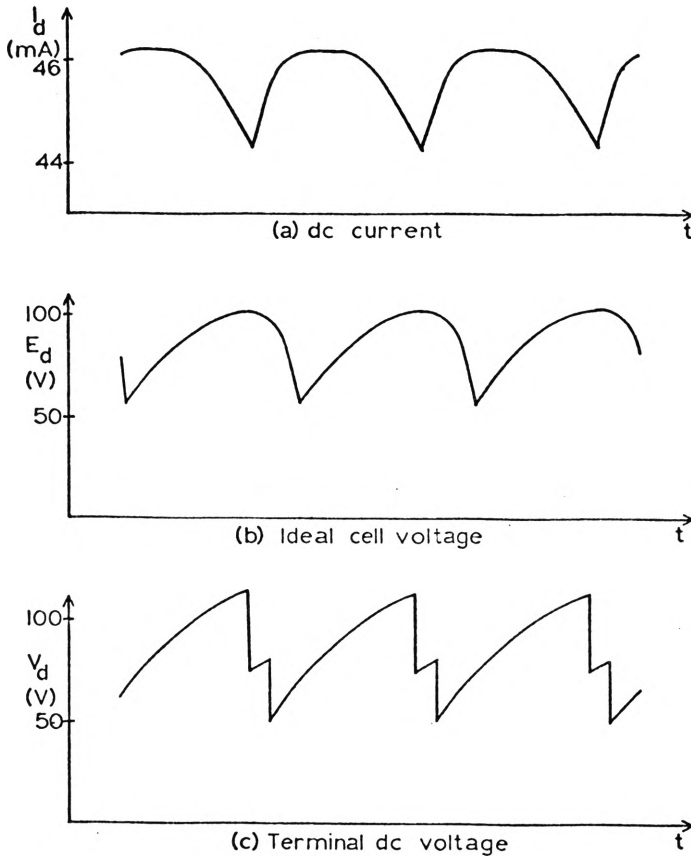


Fig. 6. Approximate steady state waveforms under CIA control, $\alpha = 137^\circ$.

variations in I_d when attempting to operate at high inverter efficiency (89% in this case) can be observed. Also, the abrupt variations in V_d (Figure 6c) at the

switching instants can be observed. This waveform can be compared with Figure 4c. The short "transition intervals" visible in Figure 6b are due to the nonzero commutation angle.

The effect that variations of the control parameters (α_{set} , I_{set} , δ_{set} and R_{set}) under their respective control modes (CIA, CCC, CEA and CRC) have on the inverter efficiency can be observed in Table I. (Due to numerical errors and finite settling times all efficiencies subject to about 2% errors.) It can be observed from this table that, under the proper circumstances, all control modes can result in a commutation failure or at least a change in mode to prevent one. The relatively wide range of settings that result in acceptable operation in the CRC mode can be observed, as well as the range of settings acceptable in the CCC mode under similar conditions.

Tables II through IV illustrate the effect of variations in the system voltage E , temperature T and solar intensity G in each of the control modes under the basic parameter settings (shown underlined in

Table I. Inverter efficiency vs. control parameter setting (fixed operating conditions).

Mode	Parameter Setting/Efficiency						
CIA	α_{set} (deg)	108	130	<u>137</u>	144	151	156
	η_{inv} (%)	< 40	77	89	96	99	*
CCC	I_{set} (mA)	44	44.5	45	<u>45.5</u>	46	47
	η_{inv} (%)	*	99	95	93	85	< 40
CEA	δ_{set} (deg)	108	136	<u>144</u>	151	158	180
	η_{inv}	< 40	80	88	94	99	*
CRC	R_{set} (Ω)	1000	1500	<u>2000</u>	2360	2560	3000
	η_{inv} (%)	55	75	94	98	99	*

*Commutation failure results (unless mode can be changed).

Table II. Change in inverter efficiency vs. system voltage level

Mode	Voltage Level E (Volts)		
	45	49	53
CIA	-8	0	+6
CCC	-5	0	-4
CEA	-9	0	+7
CRC	-6	0	-1

Table III. Change in inverter efficiency vs. temperature

Mode	Temperature (°K)	
	300	330
CIA	0	+11
CCC	0	-12
CEA	0	+13
CRC	0	+ 5

Table IV. Inverter efficiency vs. solar intensity

Mode	1200	1350	1500
CIA	-10	0	-1
CCC	<-50	0	*
CEA	0	0	-1
CRC	-12	0	-1

 * Commutation failure results

Table I). The overall observation from these tables is that (at least under the conditions given) the CCC mode is far too sensitive to variations in solar intensity to be of practical importance. The CIA and CEA mode are simple, yet they offer a somewhat wider range with acceptable performance; CEA is generally preferable for its reduced likelihood of misoperation. It may be observed that both these modes were somewhat sensitive to variations in E and T. The CRC mode resulted in the best overall steady state operation due to its

relative insensitivity to errors. Both the CCC and CRC modes, however, require careful selection of the feedback gains to prevent feedback loop instabilities and provide adequate settling times.

SUMMARY

This paper has demonstrated by means of a digital model that high inverter efficiencies can be achieved by direct three phase inversion of power from solar cell arrays. This suggests that this approach could become the primary utilization mode for solar cells should they become competitive with the ever-increasing costs of other forms of electric generation. This study has also emphasized the importance of adequate design and control of the inverter and related hardware. The controlling policy for the inverter must be dependent on the operating conditions, and the characteristics of four different controlling policies have been evaluated under a variety of conditions. Additional questions that deserve further investigation are the feasibility of real-time self-optimizing inverter controllers, the study of inverter failure modes, the analysis of filtering requirements, and the evaluation of the impact of large amounts of intermittent power generators on the power system.

REFERENCES

1. A. Bhaskara Rao and G. R. Padmanabhan, A Method for Estimating the Optimum Load Resistance of a Silicon Solar Cell Used in Terrestrial Power Applications. *Solar Energy* 15, pp. 171-177 (1973).
2. J. J. Loferski, Recent Research on Photovoltaic Solar Energy Converters. *Proc. IEEE* 51, pp. 667-674 (1963).
3. E. L. Ralph, Use of Concentrated Sunlight with Solar Cells for Terrestrial Applications. *Solar Energy* 10, pp. 67-71 (1966).

4. P. A. Berman, Design of Solar Cells for Terrestrial Use. *Solar Energy* 11, pp. 180-185 (1966).
5. S. W. Angrist, Direct Energy Conversion. Allyn and Bacon, Boston (1965).
6. M. Altman, Elements of Solid-State Energy Conversion, Van Nostrand-Reinhold, New York (1969).
7. M. Wolf and H. Rauschenbach, Series Resistance Effects on Solar Cell Measurements. *Advanced Energy Conversion*, pp. 455-479, Pergamon Press, Great Britain (1963).
8. E. W. Kimbark, Direct Current Transmission, Vol. I. Wiley, New York (1971).
9. A. H. Eltimsahy, F. L. Alvarado, T. W. Boyd, The Impact of Direct Coupling of Solar Cell Arrays to Electric Power Networks. UMR-MEC Conference on Energy, October 7-9, 1975.